Digital Filters Using Observers Applied to ICBM Control System Design

J. M. JOHNSON JR.*
Rockwell International Corp., Anaheim, Calif.

Digital filters based on state-space methods are developed whereby an "observer" is used to provide estimates of system state variables. Selected observer estimates, with appropriate gains, become the feedback control signal for the system. Procedures for independently setting the closed-loop poles of the plant and observer are outlined. Missile performance is assessed at critical flight cases. The stabilization loop is first analyzed with results presented in terms of sample calculations and time responses obtained from digital simulations for various observer/plant closed-loop pole locations. The problem of vehicle flexibility is also discussed and an observer design for bending control is outlined. The multivariable input/output observer design is treated upon closure of the steering loop around the stabilization loop.

Nomenclature

a = $V_a/57.3$
c.g. = missile center-of-gravity body station, ft
c.p. = missile center-of-pressure body station, ft; point where the resultant of all aero forces assumed to act
m = missile mass, slugs
p = first bending mode damping term = $\zeta\omega_n$
q = dynamic pressure, lb/ft^2
r = e^{-pT_s}
s = Laplace transform
S = reference area, ft^2
T = thrust, lb
x = missile states
y = measured missile states
Z = transform = e^{sT_s}
β = $(T-F_a+N_z)/mV_a$
α = angle of attack, deg
γ = flight path angle, deg = $\theta+\alpha$
θ = pitch attitude angle, deg
ψ = lateral plane attitude angle, deg
ζ = first bending mode damping ratio
τ = $[m(A_x^2+A_z^2)^{1/2}+N_z]/mV_a$
A_x, A_y, A_z = acceleration in x, y, and z trajectory directions, ft/sec^2
B_2 = $-T/mV_a$
B_3 = μ_c
b_1, b_2, etc. = gain terms, compensator
C_{n_z} = aerodynamic force coefficient
F_a = aerodynamic axial force, lb = qSC_D
I_{yy} = missile pitch inertia, ft-lb-sec^2
N_α = aerodynamic normal force per degree = qSC_{n_z}
Q_1 = first bending mode deflection, ft
T_s = sampling time, sec
V_a = velocity relative to air mass, fps
V_n = normal velocity in pitch plane, fps
V_y = normal velocity in lateral plane, fps
α_1, α_2, etc. = gain term, compensator
δ_N = nozzle deflection, deg
μ_α = qSC_{n_z}(c.g.-c.p.)$/I_{yy}$(1/sec^2)
μ_c = $\mu_c = T(X_n-\text{c.g.})/I_{yy}$
ϕ_{g_1} = first bending mode displacement, ft/ft (at nozzle hinge line)
ϕ_{l_1} = first bending mode displacement, ft/ft (at sensing device location)
λ_{g_1} = first bending mode slope, rad/ft (at sensing device location)
ω_d = first bending mode damped frequency, rad/sec
ω_n = first bending mode natural frequency, rad/sec
γ_1, γ_2 = arbitrarily selected gain values

Presented as Paper 73-845 at the AIAA Guidance and Control Conference, Key Biscayne, Fla., August 20–22, 1973; submitted September 18, 1973; revision received March 25, 1974.
Index categories: Navigation, Control, and Guidance Theory; LV/M Dynamics and Control.
* Technical Specialist.

Introduction

THE first operational digital flight control system was introduced in the Minuteman Ballistic Missile application in the early 1960's. Since this initial introduction, digital flight control has slowly gained acceptance in other areas. This slowness in acceptance has been primarily due to the high cost of digital computers and the requirements for fail-safe, fail operational control systems. These considerations were not present in the initial ballistic missile application since control and guidance calculations were time-shared and no control system redundancy was required.

For future applications, acceptance of digital flight control is expected to gain momentum because of the changes presently occurring in computer technology. These changes are producing significant cost and size reductions which will ultimately allow for the use of small dedicated General Purpose (GP) computers for control purposes only. Dedicated computers will provide the control system designer with more versatility than is generally available in a time-shared operation. In the latter, certain control laws or control changes of significance may or may not be possible to implement because of restrictions imposed by the requirement to interweave several computational programs. Changes that can be implemented may, in some instances, require the complete restructuring of the total digital computer program.

As a possible additional tool for increasing the versatility of control system designers, the technique of digital filters using observers is examined in this paper. The observer technique allows the control system designer to set closed loop system poles a priori instead of a posteriori as in conventional methods.

Missile Model

The dynamic model of the missile was derived from the perturbated set of equations of motion in the pitch plane represented in Table 1. From missile symmetry, the elimination of the gravity term ($g\cos\gamma$), and the substitution of $(T-F_A)/m$ for $(A_x^2+A_z^2)^{1/2}$ the yaw plane equations are obtained.

Data approximating a Minuteman-type ballistic missile were used. Two first stage flight cases were examined; maximum u_z/u_c and maximum u_c (missile statically unstable in both cases).

State Space Model

In state space theory, the plant is described by the state equations

$$\dot{x} = Ax + Bu \tag{1}$$

$$y = m^T x \tag{2}$$

Table 1 Missile determinant in s-plane.

EQUATION	α	θ	Q_1	V_n	δ_N
(1) Lift	$sV_a+(A_x^2+A_z^2)^{1/2}+\frac{N_\alpha}{m}$	sV_a $-g\cos\gamma$	$\frac{T\lambda_{g_1}}{m}$	0	$-\frac{T}{m}$
(2) Moment	u_α	s^2	$-u_c\lambda_{g_1}$ $T\phi_{g_1}$ $-\frac{}{I_{yy}}$	0	u_c
(3) Bending (First Mode)	0	0	$s^2+2ps+\omega_n^2$ $T\lambda_{g_1}\phi_{g_1}$ $-\frac{}{m}$	0	$\frac{T\phi_{g_1}}{m}$
(4) Normal Acceleration (Measured)	$-sV_a$	$-(cg-cp)s^2$ $-sV_a$	$57.3\phi_{I_1}s^2$	57.3s	0

where x is an n vector (representing missile states), u and y are scalars, A is the plant matrix, and B is a gain vector.

From Refs. 1 and 2, it was shown that the state equations for a sampled data system can be written as follows:

$$x_{k+1}=\Phi x_k+\Delta u_k \tag{3}$$

$$y_k=m^T x_k \tag{4}$$

$$\Phi=e^{AT_s}\text{ (transition matrix)} \tag{5}$$

$$\Delta=\int_0^{T_s}\Phi(t)B\,dt \tag{6}$$

Δ can also be determined from the partitioned matrix M as follows:

$$M=\left[\begin{array}{c:c}A & B\\ \hdashline 0 & 0\end{array}\right] \tag{7}$$

$$e^{MT_s}=\left[\begin{array}{c:c}\Phi & \Delta\\ \hdashline 0 & 1\end{array}\right] \tag{8}$$

$$u_k=-\alpha^T\hat{x}_k \tag{9}$$

where T_s is sampling time in seconds.

Also, from Ref. 1 the observer equations are given by

$$\hat{x}_{k+1}=(I-bm^T)\Phi\hat{x}_k+by_{k+1}\quad\text{open loop} \tag{10}$$

$$\hat{x}_{k+1}=(I-bm^T)(\Phi-\Delta\alpha^T)\hat{x}_k+by_{k+1}\quad\text{closed loop} \tag{11}$$

[Equation (11) defines dynamics of compensator.]

The output of a digital compensator is u_k and it contains estimates of selected plant states as determined by a discrete time observer. These observer estimates, with appropriate gains, become the control signal for the system.

The measured output variable of the plant is y_k and it serves as the input to the compensator after being sampled at a constant sampling time equal to T_s.

In closed-loop form, the Z-transform plant-observer characteristic equation from Refs. 1 and 2 can be separated into two functions as shown by Eq. (12).

$$\underset{\text{Plant}}{|ZI-(\Phi-\Delta\alpha^T)|}\quad\underset{\text{Observer}}{|ZI-(I-bm^T)\Phi|} \tag{12}$$

Briefly stated, the design technique is to: 1) set the closed-loop poles of the plant $(\Phi-\Delta\alpha^T)$ to give the desired low frequency response; and 2) set the closed-loop poles of the observer $(I-bm^T)\Phi$ for satisfactory high frequency performance.

Table 2 Missile parameters

Parameter	Flight Case: $\frac{u_\alpha}{u_c}$ Max	Flight Case: u_c Max
B_2	-0.03	-0.02
B_3	10	20
$\beta\approx\tau$	0.1	0.05
u_α	10	5
Transfer Function θ/δ_N (Rigid Body)	$\frac{10(s+0.125)}{s(s-3.16)(s+3.16)}$	$\frac{20(s+0.055)}{s(s+2.24)(s-2.24)}$
Transfer Function θ/δ_N Rigid Body + 1st BM	$\frac{-16.3(s+37)(s-37)(s+0.125)}{s(s-3.16)(s+3.16)(s^2+s+2250)}$	

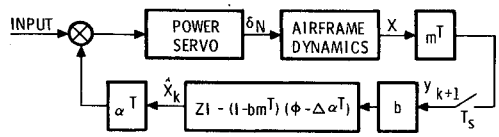

Fig. 1 Control system in state-space form.

Stabilization Control (Position and Rate Loops)

A control requirement is to design a stable system with acceptable transient characteristics in terms of rise time and overshoot in response to a step input.

Procedure

From the rigid body missile model described in Table 1, Eq. (1) in matrix form becomes

$$\begin{bmatrix}\dot{\theta}\\ \dot{\alpha}\\ \ddot{\theta}\end{bmatrix}=\begin{bmatrix}0 & 0 & 1\\ 0 & -\tau & -1\\ 0 & u_\alpha & 0\end{bmatrix}\begin{bmatrix}\theta\\ \alpha\\ \dot{\theta}\end{bmatrix}+\begin{bmatrix}0\\ -\frac{T}{mV_a}\\ \mu_c\end{bmatrix}\delta_N \tag{13}$$

Table 2 represents the parametric values of the missile for two selected flight cases.

The object is to determine the b's and α's in Fig. 1 for specific pole locations. From Eq. (12) the observer characteristic equation is given by

$$|ZI-(I-bm^T)\Phi| \tag{14}$$

and the plant characteristic equation is given by

$$|ZI-(\Phi-\Delta\alpha^T)| \tag{15}$$

Since the angle of attack is essentially equal and opposite to the attitude angle during the first few seconds of the transient response, a simplified second-order observer will suffice. The outputs of the observer are estimates of the attitude angle and attitude rate. Because the observer is second-order and the plant third-order, only two closed-loop plant poles can be directly controlled. The final location of the indirectly controlled pole depends upon the over-all open-loop pole-zero configuration of the total system.

Using θ (missile attitude) as the measured output variable $(y=m^Tx)$ and expanding Eq. (14) for a second-order observer with

$$(I-bm^T)\Phi=\begin{bmatrix}1-b_1 & T_s(1-b_1)\\ -b_2+u_\alpha T_s & 1-b_2T_s\end{bmatrix} \tag{16}$$

yields the following in terms of the unknown b's:

$2-b_1-b_2T_s=$ sum of the two preselected observer pole roots in Z-plane (17)

$(1-b_1)(1-u_\alpha T_s^2)=$ product of the two preselected observer pole roots in Z-plane

Expanding Eq. (15) with $\Phi-\Delta\alpha^T$ equal to

$$\begin{bmatrix}1-\Delta_1\alpha_1 & T_s-\Delta_1\alpha_2\\ u_\alpha T_s-\Delta_2\alpha_1 & 1-\Delta_2\alpha_2\end{bmatrix} \tag{18}$$

where

$$\Delta_1=(T_s^2/2)u_c$$
$$\Delta_2=T_su_c \tag{19}$$

yields the following in terms of the unknown α's:

$2-\Delta_2\alpha_2-\Delta_1\alpha_1=$ sum of the two preselected plant pole roots in Z-plane (20)

$1-u_\alpha T_s^2+\alpha_1(T_s\Delta_2-\Delta_1)+\alpha_2(u_\alpha T_s\Delta_1-\Delta_2)=$ product of the two preselected plant pole roots in Z-plane

At this point various observer pole locations are selected in combination with a selected set of plant poles to yield the

desired over-all system response, e.g., in terms of minimum rise time and overshoot. Obviously, a large number of observer pole locations in the stable region are possible but only the regions of high frequency relative to the short period frequency are considered practical.

Knowing the short period frequency (generally about $\frac{1}{3}$ to 1 cycle), various observer pole locations of higher frequency are selected, the b's calculated and digital simulation runs made of the system shown in Fig. 1 to determine acceptable observer/plant pole combinations to satisfy specific system requirements. The process is repeated for other observer/plant pole combinations as necessary. The simulation runs are made with the equations in matrix form; therefore, there is no need to compute the compensator transfer function. However, because it generally will be desired for reasons of computer programing and/or for correlation of time and frequency domain analyses, the procedures for obtaining the transfer function are outlined.

First, we take the Z transform of Eq. (11) which yields

$$\hat{x}(Z) = (I - \Phi_F Z^{-1})^{-1} b y(Z) \tag{21}$$

where

$$\Phi_F = (I - bm^T)(\Phi - \Delta\alpha^T) \tag{22}$$

Multiplying Eq. (21) by α^T gives the feedback control signal

$$u(Z) = \alpha^T \hat{x}(Z) \tag{23}$$

Combining Eqs. (22) and (23) the compensator transfer function becomes

$$u(Z)/y(Z) = \alpha^T (I - \Phi_F Z^{-1})^{-1} b \tag{24}$$

Substituting for the inverse function[3] we have

$$\frac{u(Z)}{y(Z)} = \alpha^T \frac{\text{adjoint}\,(ZI - \Phi_F) bZ}{|ZI - \Phi_F|} \tag{25}$$

where the compensator poles are given by

$$|ZI - \Phi_F| \tag{26}$$

and the compensator zeros by

$$\alpha^T \text{ adjoint}\,(ZI - \Phi_F) b \tag{27}$$

Equation (27) can be simplified if we let

$$Q(Z)/P(Z) = (ZI - \Phi_F)^{-1} \tag{28}$$

where

$$P(Z) = Z^N - P_1 Z^{N-1} - P_2 Z^{N-2} \cdots P_N \tag{29}$$

$$Q(Z) = C_0 Z^{N-1} + C_1 Z^{N-2} + C_2 Z^{N-3} \cdots + C_{N-1} \tag{30}$$

and the coefficients are defined by the Method of Faddeev[4] as follows:

$$\begin{gathered} \Phi_{F_i} = \Phi_F C_{i-1} \qquad C_0 = I \qquad P_i = (1/i)(\text{trace } \Phi_{F_i}) \\ i = 1, N \qquad C_i = \Phi_{F_i} - P_i I \end{gathered} \tag{31}$$

For a second-order compensator Eq. (27) becomes

$$\alpha^T b Z - \alpha^T C_1 b \tag{32}$$

From Eq. (31) we note that

$$C_1 = \Phi_F - \text{trace}\,(\Phi_F) \tag{33}$$

Substituting Eq. (22) into Eq. (33) and substituting the result for C_1 in Eq. (32) gives

$$\alpha^T C_1 b = \alpha^T (\Phi - tr\,\Phi) b$$

$$\begin{pmatrix} +\alpha^T bm^T \Delta\alpha^T b + \alpha^T bm^T \Phi b + \alpha^T b \alpha^T \Delta \\ -\alpha^T bm^T \Phi b - \alpha^T \Delta\alpha^T b - \alpha^T bm^T \Delta\alpha^T b \end{pmatrix} = 0 \tag{34}$$

Therefore, the numerator function becomes

$$\alpha^T [\text{adj}\,(ZI - \Phi)] b \tag{35}$$

In other words, to solve for the zeros it is only necessary to calculate the adjoint of $ZI - \Phi$ instead of the adjoint of the more complicated $ZI - \Phi_F$ function. Equation (35) is a general solution that holds for any order function.

Sample Calculations and Results (u_α/u_c max flight case)

The following assumptions were made: 1) actuation transfer function of unity was used since servo frequency considerably higher ($>10:1$) than short period frequency; and 2) sampling time of 0.03 sec used (0.03–0.06 sec generally acceptable).

The observer is second order, therefore, two poles are selected. Substituting pole locations corresponding to

$$(e^{-20T_s} \text{ and } e^{-20T_s}) \text{ into Eq. (17)}$$

yields

$$\begin{aligned} b_1 &= 0.696 \\ b_2 &= 6.88 \end{aligned} \tag{36}$$

Substituting plant poles of $e^{-(4 \pm j2)T_s}$ and

$$\Delta = \begin{bmatrix} 0.0045 \\ 0.3 \end{bmatrix} \tag{37}$$

into Eq. (20) yields

$$\begin{aligned} \alpha_1 &= 2.665 \text{ (attitude gain)} \\ \alpha_2 &= 0.7245 \text{ (attitude rate gain)} \end{aligned} \tag{38}$$

The compensator transfer function is solved in two parts, the zero from Eq. (35) and the poles from Eq. (26). The Φ function is given by

$$\Phi = \begin{bmatrix} 1 & 0.03 \\ 0.3 & 1 \end{bmatrix} \tag{39}$$

Substituting Eqs. (36, 38, and 39) into Eq. (35) yields a numerator of

$$6.839(Z - 0.8975) \tag{40}$$

Expanding Eq. (22) where

$$I - bm^T = \begin{bmatrix} 0.304 & 0 \\ -6.88 & 1 \end{bmatrix} \tag{41}$$

and

$$\Phi - \Delta\alpha^T = \begin{bmatrix} 0.988 & 0.02674 \\ -0.4995 & 0.78265 \end{bmatrix} \tag{42}$$

gives

$$|ZI - \Phi_F| = Z^2 - 0.899Z + 0.239 \tag{43}$$

Combining Eqs. (40) and (43) the transfer function of the compensator is

$$6.839(Z - 0.8975)/(Z^2 - 0.899Z + 0.239) \tag{44}$$

with steady-state gain = 2.06 for the selected observer/plant poles.

In general, the technique of preselecting observer and plant poles results in a compensator steady-state gain greater than unity as indicated by Eq. (44) (designated K_c; see Fig. 2). In order for the output θ to approach a steady-state value of unity in response to a unit step command, the compensator steady-state gain is adjusted to unity and the forward-loop gain increased by the inverse of the compensator gain adjustment.

Figures 2 and 3 are plots of attitude angle overshoot and rise time vs compensator steady-state gain, respectively, of the u_α/u_c max flight case as a function of observer poles for a selected set of plant pole locations. Other combinations of

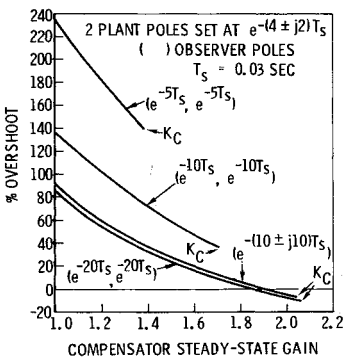

Fig. 2 Percent overshoot in response to unit step vs compensator steady-state gain as a function of observer poles for u_α/u_c max flight case.

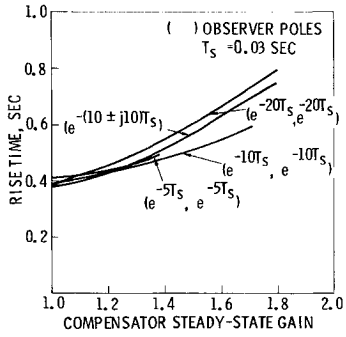

Fig. 3 Rise time in response to unit step vs compensator steady-state gain as a function of observer poles for u_α/u_c max flight case.

observer/plant pole locations would similarly be plotted for the same flight case as well as other critical flight cases in order to select the "best" compensator.

From Figs. 2 and 3 several observer pole locations, e.g., e^{-20T_s}, e^{-20T_s}, and $e^{-(10 \pm j10)T_s}$ are acceptable for the selected plant pole locations. As the steady-state compensator gain increases, the percent overshoot decreases and the rise time increases; however, θ steady-state approaches the reciprocal of the compensator steady-state gain. Figure 4 shows the transient response of θ and its sampled estimate for observer poles of (e^{-20T_s}, e^{-20T_s}) with a steady-state compensator gain of unity. The selected closed-loop plant poles are located at $e^{-(4 \pm j2)T_s}$. The time response is considered acceptable from the standpoint of overshoot and rise time although the settling time is long. This occurs because the third plant pole (the pole being indirectly controlled) approaches the plant zero (see Table 2) giving the effect of a long time constant integrator. This characteristic is not considered critical because the vehicle is in a continuous dynamic-state; therefore, the criteria for compensator selection is based mainly on the characteristics of minimum overshoot coupled with a fast rise time.

Figure 5 is for the same flight case as Fig. 4 except the plant poles were located at $e^{-(2 \pm j2)T_s}$. This reduced the α_1 and α_2 gains to 1.9512 and 0.4445, respectively. The rise time characteristics of the two figures are similar; however, Fig. 5 exhibits the larger overshoot (157% vs 87%), indicating the undesirability of lower damping on the plant poles.

In general, a summary of the results from all the critical flight cases will indicate that a constant set of b's and α's for each stage of flight is feasible; however, in some instances it may be desired to introduce an α gain change at some specific point in the trajectory to improve the over-all system stability margins.

Rigid Body Plus Bending Analyses

When the effects of bending (first mode only shown) are added to the simplified two-dimensional rigid body model, the over-all missile model becomes

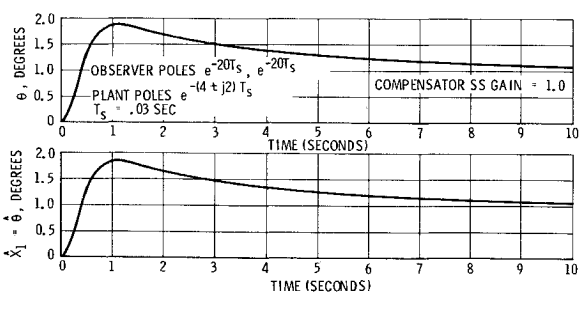

Fig. 4 Attitude and attitude estimate time response to unit step input for u_α/u_c max flight case.

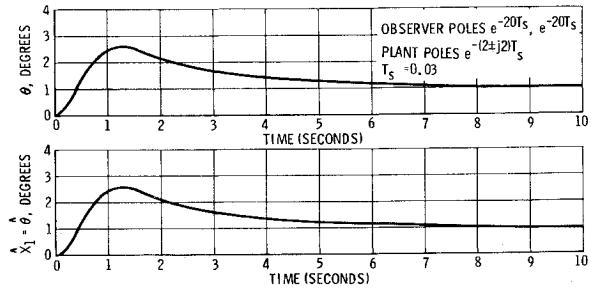

Fig. 5 Attitude and attitude estimate time response to unit step input for u_α/u_c max flight case (plant poles different from Fig. 4).

$$\begin{bmatrix} \dot{\theta} \\ \ddot{\theta} \\ \dot{Q}_1 \\ \ddot{Q}_1 \end{bmatrix} = \begin{bmatrix} 0 & 1 & 0 & 0 \\ u_\alpha & 0 & 0 & 0 \\ 0 & 0 & 0 & 1 \\ 0 & 0 & -\omega_n^2 & -2p \end{bmatrix} \begin{bmatrix} \theta \\ \dot{\theta} \\ Q_1 \\ \dot{Q}_1 \end{bmatrix} + \begin{bmatrix} 0 \\ u_c \\ 0 \\ \dfrac{T\phi_{g1}}{m} \end{bmatrix} \delta_N \quad (45)$$

In order to facilitate the calculation of the transition matrix Φ, Eq. (45) is modified by remodeling the bending portion of the matrix to a symmetric form which requires a change in one of the bending states as indicated by Eq. (46).

$$\begin{bmatrix} \dot{\theta} \\ \ddot{\theta} \\ \dot{Q}_1 \\ \dfrac{p}{\omega_d}\dot{Q}_1 + \dfrac{\ddot{Q}_1}{\omega_d} \end{bmatrix} = \begin{bmatrix} 0 & 1 & 0 & 0 \\ u_\alpha & 0 & 0 & 0 \\ 0 & 0 & -p & \omega_d \\ 0 & 0 & -\omega_d & -p \end{bmatrix} \begin{bmatrix} \theta \\ \dot{\theta} \\ Q_1 \\ \dfrac{p}{\omega_d}Q_1 + \dfrac{\dot{Q}_1}{\omega_d} \end{bmatrix} + \begin{bmatrix} 0 \\ \mu_c \\ 0 \\ \dfrac{T\phi_{g1}}{m} \end{bmatrix} \delta_N \quad (46)$$

Bending excitation accompanying the control signal is considered synonymous with noise and therefore is unwanted. Bending control on a Minuteman-type ballistic missile is accomplished by passive techniques which tend to decouple the bending frequencies from the basic control signal. The bending frequencies and damping are not directly controlled but stabilization/decoupling is accomplished by: 1) proper location of rate instrument with filtering; and 2) digital differentiation of attitude information with filtering.

The second method is presently being used in Minuteman and will serve as the basis for the observer design.

Equation (46) is used to model the observer, thus a fourth-order compensator is required. This involves the computation of new b's upon selection of four closed-loop poles, two of which can remain as previously selected for the rigid body case. The other two poles are arbitrarily located in the left half plane, generally some distance from the compensator zeros. In essence, the compensator is a notch filter in the vicinity of the first bending mode frequency, thereby minimizing the bending effects on the $\hat{x}_1$ and $\hat{x}_2$ rigid body signals. To obtain an equation for the new b's, the function $(I - bm^T)\Phi$ is expanded and b's calculated to satisfy preselected pole selections where

$$I - bm^T = \begin{bmatrix} 1-b_1 & 0 & -b_1 & 0 \\ -b_2 & 1.0 & -b_2 & 0 \\ -b_3 & 0 & 1-b_3 & 0 \\ -b_4 & 0 & -b_4 & 1.0 \end{bmatrix} \quad (47)$$

and

$$\Phi = \begin{bmatrix} 1 & T_s & 0 & 0 \\ u_\alpha T_s & 1 & 0 & 0 \\ 0 & 0 & e^{-pT_s}\cos(\omega_d T_s) & e^{-pT_s}\sin(\omega_d T_s) \\ 0 & 0 & -e^{-pT_s}\sin(\omega_d T_s) & e^{-pT_s}\cos(\omega_d T_s) \end{bmatrix} \quad (48)$$

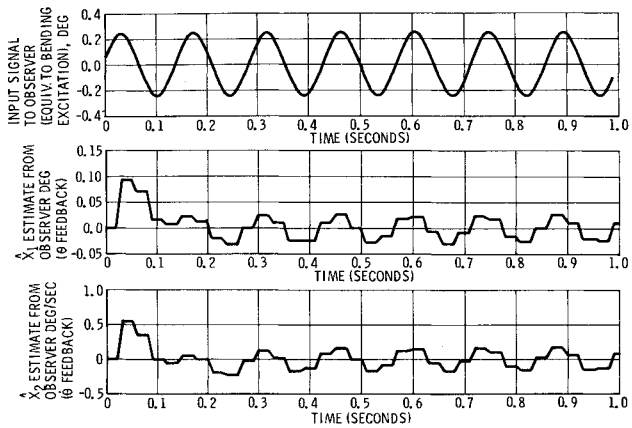

Fig. 6 Response of bending notch filter to bending excitation signal input.

where p and ω_d can be selected values that approximate the average damping term and damped frequency of the first bending mode during the first stage of flight. In general, it has been found that a constant notch filter is acceptable for an ICBM.

The α's would remain as previously computed for the rigid body case, since the closed-loop plant pole settings remain unchanged. The zeros of the compensator are determined from Eq. (35). The Φ matrix can be partitioned as shown by Eq. (49)

$$\Phi = \begin{bmatrix} \Phi_a & \vdots & 0 \\ \cdots & \vdots & \cdots \\ 0 & \vdots & \Phi_b \end{bmatrix} \tag{49}$$

Using Eq. (49) the adjoint $(ZI-\Phi)$ becomes

$$\begin{bmatrix} (ZI-\Phi_a)^{-1} & \vdots & 0 \\ \cdots & \vdots & \cdots \\ 0 & \vdots & (ZI-\Phi_b)^{-1} \end{bmatrix} |ZI-\Phi_a|\,|ZI-\Phi_b| \tag{50}$$

From Eq. (50), Eq. (35) becomes

$$|ZI-\Phi_a|\,|ZI-\Phi_b|\alpha_{1,2}^T(ZI-\Phi_a)^{-1}b \tag{51}$$

since α_3 and α_4 are zero. Substituting for $(ZI-\Phi_a)^{-1}$, Eq. (51) becomes

$$|ZI-\Phi_b|\alpha_{1,2}^T[\text{adj}\,(ZI-\Phi_a)]b_{1,2} \tag{52}$$

The notch zeros are given by $|ZI-\Phi_b|$ which reduces to the form

$$Z^2-2r\cos(\omega_d T_s)Z+r^2 \tag{53}$$

where ω_d is the tuned frequency of the notch and r controls the sharpness of the notch. The closer r is to unity, the sharper the notch.

The remaining compensator zero is determined from

$$\alpha_{1,2}^T[\text{adj}\,(ZI-\Phi_a)]b_{1,2} \tag{54}$$

Sample Bending Filter Response

Representative values of $p = 0.1$, $\omega_d = 40$ rad/sec, observer poles of $e^{-(30\pm j30)T_s}$, e^{-20T_s}, and e^{-10T_s} were selected and the b's digitally computed to be

$$\begin{aligned} b_1 &= 0.3907 \\ b_2 &= 2.262 \\ b_3 &= 0.5404 \\ b_4 &= 0.2996 \end{aligned} \tag{55}$$

Figure 6 shows the response of the notch filter when an assumed sinusoidal bending signal of 45 rad/sec is applied as the input to the observer. Based on the frequencies involved the filter is detuned approximately 10%. The decoupling effectiveness of the filter can be seen since less than 10% of the bending input signal appears in the estimates of $\hat{x}_1$ and $\hat{x}_2$ which are the normal feedback signals representing vehicle attitude and attitude rate, respectively.

Stabilization plus Steering Loop, Multivariable Control (Yaw Plane) Integrated Control

The steering loop is closed around the inner stabilization loop discussed previously. In the ICBM application it is desired to hold the lateral acceleration and velocity to zero, while in the pitch plane the vehicle follows steering commands as generated by the guidance system. In the lateral plane (yaw) the measured variables are the yaw attitude angle and the lateral velocity as determined from the Inertial Measuring Unit (IMU). Thus, the signal to the observer will be a multivariable input consisting of attitude angle and lateral velocity. In the initial design phase it is generally desirable to first conduct an analog design to "ballpark" the design parameters. Therefore, the procedures are first presented for the analog design followed by the digital design based on the results of the "best" analog observer.

Analog System Analysis

To form the basis for the design, a signal flow diagram of the lateral system is established in terms of acceleration, lateral velocity, angular acceleration, attitude rate, and attitude (angle of attack eliminated from equations of motion). Figure 7 is a system flow diagram in analog form of the lateral system.

Figure 8 shows the lateral system in block diagram form. The state matrix A in analog form is given by

$$\begin{bmatrix} \dot{\psi} \\ A_y \\ \ddot{\psi} \\ \dot{x}_4 \end{bmatrix} = \begin{bmatrix} 0 & 0 & 1 & 0 \\ a\beta & -\beta & 0 & -(T/mV_a)a \\ u_\alpha & -u_\alpha/a & 0 & u_c \\ 0 & 0 & 0 & 0 \end{bmatrix} \begin{bmatrix} \psi \\ V_y \\ \dot{\psi} \\ x_4 \end{bmatrix} \tag{56}$$

where the x_4 state is equivalent to a Ψ_c step command to the plant.

The compensator equation in analog form is indicated by

$$\dot{\hat{x}} = (A-bm^T-B\alpha^T)\hat{x}+by \tag{57}$$

where

$$y = m^T x = \begin{bmatrix} 1 & 0 & 0 & 0 \\ 0 & 1 & 0 & 0 \end{bmatrix} x$$

The plant poles are set by the function

$$|sI-(A-B\alpha^T)| \tag{58}$$

and the observer poles by the function

$$|sI-(A-bm^T)| \tag{59}$$

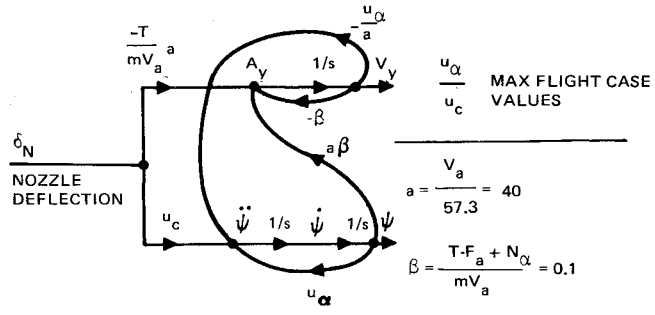

Fig. 7 Signal flow diagram of lateral system (no control feedback).

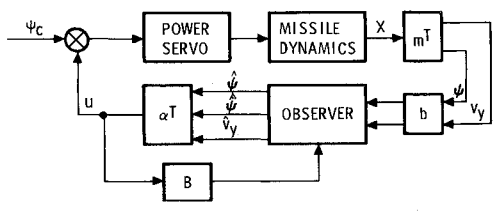

Fig. 8 Block diagram of lateral system (analog).

Expanding bm^T we have

$$\begin{bmatrix} b_{11} & b_{12} & 0 & 0 \\ b_{21} & b_{22} & 0 & 0 \\ b_{31} & b_{32} & 0 & 0 \\ b_{41} & b_{42} & 0 & 0 \end{bmatrix} \tag{60}$$

Substituting Eqs. (56) and (60) into Eq. (59) and expanding, results in a nonlinear equation in b's, since product terms result. To linearize the system, Eq. (60) is rewritten as follows:

$$\begin{bmatrix} b_1 \\ b_2 \\ b_3 \\ b_4 \end{bmatrix} [\gamma_1 \quad \gamma_2] \begin{bmatrix} 1 & 0 & 0 & 0 \\ 0 & 1 & 0 & 0 \end{bmatrix} \tag{61}$$

which results in four unknown b's since the γ's can be arbitrarily selected. Substituting Eqs. (56) and (61) into Eq. (59) and expanding, the result yields the following in terms of the unknown b's:

$\gamma_1 b_1 + \gamma_2 b_2 =$ sum of the four preselected observer pole roots in s-plane $- \beta$

$(a\beta\gamma_2 + \beta\gamma_1)b_1 + \gamma_1 b_3 + B_2 a\gamma_2 b_4 =$ sum of products of the four preselected observer pole roots in s-plane taken two at a time $+ u_\alpha$

$$\left(-\frac{u_\alpha \gamma_1}{a} - u_\alpha \gamma_2\right) b_2 + (a\beta\gamma_2 + \beta\gamma_1)b_3 + B_3\gamma_1 b_4 =$$

sum of products of the four preselected observer pole roots in s-plane taken three at a time

$[B_3(\beta\gamma_1 + a\beta\gamma_2) - B_2(au_\alpha\gamma_2 + u_\alpha\gamma_1)]b_4 =$ product of the four preselected observer pole roots in s-plane

To determine the α gains, closed-loop poles are selected and Eq. (58) expanded. To cancel the step input in the outer loop (considered a disturbance), it is desired to have an integrator in the compensator. This is accomplished when $\alpha_4 = 1.0$ which makes the fourth column of the $A - bm^T - B\alpha^T$ matrix zero.

Expanding Eq. (58) with $\alpha_4 = 1.0$ yields the following in terms of the unknown α's:

$B_2 a\alpha_2 + B_3\alpha_3 =$ sum of the three preselected plant pole roots in s-plane $- \beta$

$B_3\alpha_1 + (B_3\beta - B_2 u_\alpha)\alpha_3 =$ sum of products of the three preselected plant pole roots in s-plane taken two at a time $+ u_\alpha$

$(B_3\beta - B_2 u_\alpha)\alpha_1 + (B_3 a\beta - B_2 a u_\alpha)\alpha_2 =$ product of the three preselected plant pole roots in s-plane (63)

At this point it is necessary to determine the "best" γ's to yield the desired over-all compensator/plant response characteristics. A set of three plant poles are selected and Eq. (63) solved for the α's.

Next, since the observer is fourth order, four observer poles are selected and Eq. (62) solved for the b's for arbitrarily selected γ's.

Sample System Results

Various γ values were selected, the b's calculated, and digital simulations performed to determine the γ values which resulted in the best over-all system response for the selected closed-loop plant poles. The best system response was judged to be the one with the lowest peak parameter values (ψ, A_y, V_y, α) and the smallest control or nozzle activity. Figure 9 shows the peak responses of the system parameters for the u_α/u_c max flight case as a function of the ratio γ_1/γ_2. It can be seen that a ratio of 10.0 gave the best results based on the criteria established. The over-all nozzle activity was also a minimum for this ratio. The b's and α's used in the system represented by Fig. 9 for $\gamma_1/\gamma_2 = 10$ were computed from Eqs. (62) and (63) to be as follows:

$$\begin{aligned} b_1 &= -176.8 \\ b_2 &= 2067 \\ b_3 &= 469.6 \\ b_4 &= 385 \\ \alpha_1 &= 1.55 \quad \text{(attitude gain)} \\ \alpha_2 &= 0.0382 \quad \text{(lateral velocity gain)} \\ \alpha_3 &= 0.415 \quad \text{(attitude rate gain)} \\ \alpha_4 &= 1.0 \quad \text{(integrator gain)} \end{aligned} \tag{64}$$

In the event the particular combination of compensator/plant poles selected does not yield the desired response, others are selected and the above steps repeated until the system specifications are satisfied.

Digital System Analysis

The digital design is initiated by calculating the Φ and Δ functions by setting

$$A = \begin{bmatrix} 0 & 0 & 1 \\ a\beta & -\beta & 0 \\ u_\alpha & -u_\alpha/a & 0 \end{bmatrix} \tag{65}$$

and a new B function given by

$$B = \begin{bmatrix} 0 \\ -(T/mV_a)a \\ u_c \end{bmatrix} \tag{66}$$

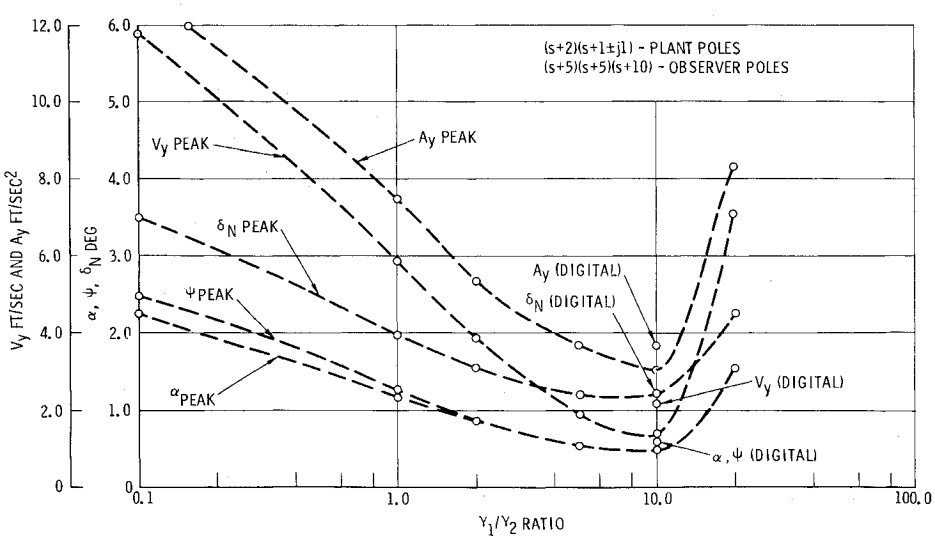

Fig. 9 γ_1/γ_2 ratio vs peak system parameters of lateral system for u_α/u_c max flight case in response to unit step ψ_c.

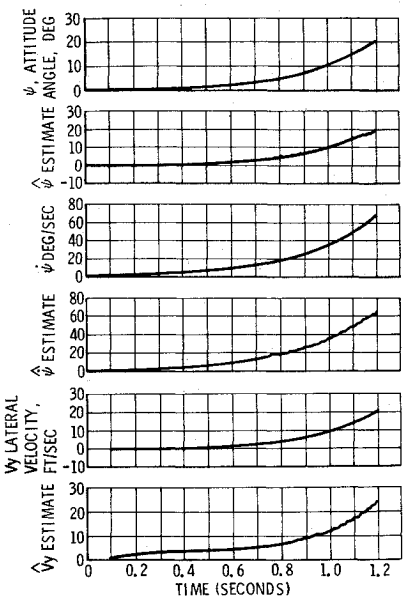

Fig. 10 Open-loop observer response for lateral system (u_α/u_c max flight case).

Substituting Eqs. (65) and (66) into Eq. (7) and solving Eq. (8) by digital computer expansion yields the desired Φ and Δ functions. The results of Eq. (8) are substituted in Eq. (12) to determine the plant-observer characteristic equation in terms of the three unknown α's (α_4 is set equal to unity as in the analog case) and the four unknown b's. To circumvent computational difficulties and for reasons of accuracy the α's and b's, are digitally computed.

Sample System Results

The sample digital results are based on transforming the "best" analog system ($\gamma_1/\gamma_2 = 10$) into the Z-plane. Transforming the observer/plant poles of Fig. 9 into the Z-plane the b's and α's were digitally computed to be

$$
\begin{aligned}
b_1 &= -0.693 \\
b_2 &= 13.84 \\
b_3 &= 8.735 \\
b_4 &= 4.189 \qquad (67)\\
\alpha_1 &= 1.523 \quad \text{(attitude gain)} \\
\alpha_2 &= 0.0341 \quad \text{(lateral velocity gain)} \\
\alpha_3 &= 0.3957 \quad \text{(attitude rate gain)}
\end{aligned}
$$

Figure 10 shows the open-loop tracking of the observer for the u_α/u_c max flight case using the above calculated b's. Good correspondence between the system variables and their observer estimates are exhibited. Figure 11 is the closed-loop response of the system shown in Fig. 10 for a unit ψ_c step. Again, as in the open-loop case, the estimates are in close correspondence with the state variables in question. The resulting closed-loop peak values of selected system parameters are indicated in Fig. 9. As expected, the digital values are slightly higher than the corresponding analog values.

Using the identical compensator and control gains of Fig. 11, time responses for other flight cases may result in longer settling times for V_y thereby causing a larger lateral displacement offset than for the u_α/u_c max flight case. If this proves undesirable, a reduction could be achieved by introducing an α gain change at some point between the two flight cases. The b gains need not be changed during the stage.

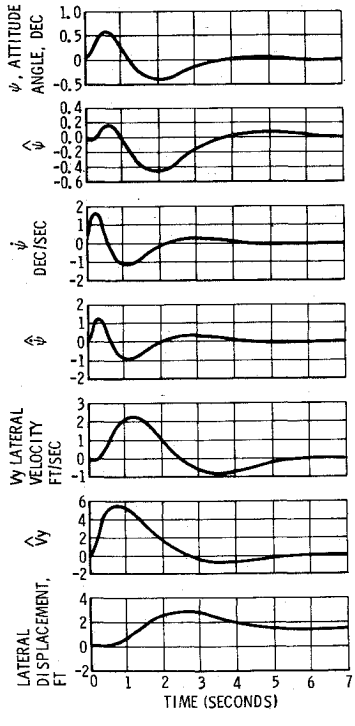

Fig. 11 Closed-loop response to ψ_c step for lateral system (u_α/u_c max flight case).

Conclusion

In this section, a procedure for using the observer technique as applied to the ballistic missile application is outlined. This is briefly summarized as follows.

Stabilization Loop (Single Input/Multivariable Output)

1) Establish criteria for system evaluation.
2) Establish plant parameters for critical flight cases.
3) Set up A, B, and M matrices.
4) Compute Φ and Δ from expansion of e^{MT_s}† (acceptable values of T_s for ballistic missiles are generally 0.03–0.06 sec).
5) Select eigenvalues for plant poles, compute α's.
6) For selected plant poles, select various observer pole locations, and compute corresponding b's.
7) Perform digital computer simulations of complete system for plant/observer pole locations to obtain time responses for evaluation. Simulation equations are solved in matrix form, therefore transfer functions are not computed as done in conventional simulations.
8) If time responses of step 7 are unacceptable, repeat steps 6 and 7 until evaluation criteria are satisfied.

Stabilization Loop plus Steering Loop (Multivariable Input/Output)

This is the same as stabilization loop analysis except an intermediate step is necessary to determine "best" ratio of b gains to apply to multivariable observer input signal.

Analog design step is desirable since it provides a convenient means to "ball-park" system parameters in the initial design phase.

References

[1] Bona, B. E., "Digital Filter Design Using Observers," *Proceedings of the Fifth Asilomar Conference on Circuits and Systems,* Naval Postgraduate School, Monterey, Calif., and Univ. of Santa Clara, Santa Clara, Calif., Nov. 1971, pp. 1–2.

[2] Luenberger, D. G., "Observing the State of a Linear System," *IEEE Transactions on Military Electronics,* Vol. MIL-8, April 1964.

[3] Franklin, J. N., *Matrix Theory,* Prentice-Hall, Englewood Cliffs, N.J., 1968, pp. 17–19.

[4] Feddeeva, V. N., *Computational Method of Linear Algebra,* Dover, New York, 1959, pp. 179–182.

† Also similar for aircraft.